Ecological Indicators 146 (2023) 109842

Contents lists available at ScienceDirect

Ecological Indicators

journal homepage: www.elsevier.com/locate/ecolind

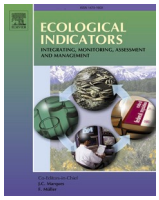

Original Articles

Tracking spatio-temporal dynamics of harmful algal blooms using long-term MODIS observations of Chaohu Lake in China from 2000 to 2021

Ting Zhou [a,b,*], Yan Li [b], Bo Jiang [c], Juha M. Alatalo [d], Chen Li [b], Cheng Ni [a]

[a] School of Engineering, Anhui Agricultural University, China
[b] East China Engineering Science & Technology Co. Ltd., China
[c] Changjiang Water Resources Protection Institute, China
[d] Environmental Science Center, Qatar University, Qatar

ARTICLE INFO

Keywords:
Harmful algal blooms (HABs) distribution
Spatio-temporal dynamics
Meteorological factor
Human activities
Floating algae index
Chaohu Lake

ABSTRACT

Harmful algal blooms (HABs) have long been a critical threat to environmental safety and health, especially in inland lakes with rapidly growing socioeconomic development. Although satellite remote sensing provides an efficient manner to observe floating algae blooms, tracing and capturing the distribution of HABs in water bodies remains challenging for their high dynamics in both spatial and temporal dimensions. This study analyzed the spatio-temporal dynamics of HABs in Chaohu Lake, China, from 2000 to 2021. Daily MODIS remote sensing observations, including 7926 images, were utilized. The Floating Algae Index (FAI) was applied to each image to detect the area and severity of HABs. Results show that the HABs in Chaohu Lake have generally been increasing in the past two decades, with two intermittent decreases in 2016–2017 and 2020–2021, and the duration of HABs tended to be longer over the years. HABs were most severe and frequent in the lake's northwestern area. Temperature and precipitation are two main meteorological factors positively correlated with HABs. The fast-growing socio-economy reflected by population and GDP increase lake eutrophication and HABs. However, environment management policies since 2020 have had a significant and rapid influence in decreasing the lake's nutrients, which greatly reduced HABs severity in 2020 and 2021. This study's results further indicate that high-frequency remote sensing observations, although with occasional data missing due to cloud cover, can still perform well in describing HABs, as long as the analysis method is appropriately adopted. This finding provides potential significance for utilizing remote sensing products, especially for highly dynamic object observation where high-quality images are lacking.

1. Introduction

For the past few decades, inland waters have faced severe challenges of HABs due to increasing human activities and global climate change (Xu et al., 2003; Wang et al., 2015; Zhang et al., 2015). HABs can last a few days to months. Frequent HABs outbreaks threaten water resources, environmental systems, human health, etc. (Liu et al., 2021; Chen et al., 2021). HABs will severely deplete oxygen levels and produce massive methane emissions with a pungent poisonous gas (Guo et al., 2021; Friedman and Levin, 2005). HABs are a greater threat to water safety and ecological health for inland urban lakes. Therefore, it is vital to observe, trace, and analyze the evolution of HABs. However, HABs can develop rapidly under optimal climatic and aquatic conditions. The severity and spatial distribution are highly dynamic, for it is sensitive to meteorological factors such as temperature, precipitation, and wind direction (Díaz et al., 2021), making it challenging to describe the detailed spatio-temporal dynamics of HABs over long periods.

Remote sensing technology provides an efficient manner to review long-term HABs development in water areas or trace the real-time condition of HABs (Coffer et al., 2021; Bosse et al., 2019). Remote sensing has a significant advantage over in situ observations due to its low cost, easy access, and traceability to the past time (Sun et al., 2016; Yuan et al., 2021). Different satellite remote sensing products have been applied in observing and analyzing HABs in water areas globally (Stroming et al.,2020; Hunter et al.,2009). Various indicators have been used to extract HABs based on remote sensing images, such as normalized difference vegetation index (NDVI) (Qin et al., 2022; Cao and Han, 2021; Teta et al., 2021), enhanced vegetation index (EVI) (Pan et al.,

* Corresponding author at: School of Engineering, Anhui Agricultural University, China.
E-mail address: zhouting@ahau.edu.cn (T. Zhou).

https://doi.org/10.1016/j.ecolind.2022.109842
Received 21 September 2022; Received in revised form 20 December 2022; Accepted 25 December 2022
Available online 29 December 2022

2012; Cong et al.,2009; Hillman et al.,2021), floating algae index (FAI) (Jia et al., 2019; Shi et al., 2019; Naghdi et al., 2018), maximum chlorophyll index (MCI) (Alikas et al., 2010) and machine learning models based on spectral band data (Song et al., 2022; Pyo et al., 2021; Li et al., 2021).

Chaohu lake has attracted numerous studies on its HABs (Zhang et al., 2015); it is one of the five largest freshwater lakes in China, is heavily affected by eutrophication, and has been prone to HABs. Previous studies have analyzed various spatial and temporal variations of HABs using different satellite remote-sensing products (Zhang et al., 2015; He et al., 2018; Ma et al., 2021). Previous studies revealed that the HABs in Chaohu Lake occurred mainly from May to November, were more frequent and severe in western parts of the lake, and have been increasing during the past few decades. However, as HABs are highly dynamic, there remain uncertainties in the general and detailed characteristics of HABs.

The driving forces of HABs growth have attracted increasing attention, as it may potentially explain the outbreak of HABs and be helpful in future water environment management (Ma et al., 2021; Qin et al., 2022; Liu et al., 2022; Zhang et al., 2021). HABs are sensitive to environmental factors and human activities. Meteorological factors commonly involve temperature, precipitation, sunshine hour, wind condition, etc.; human activity factors involve population, economic growth, land use, water management policies, etc. (Xu and Xu, 2022; Zhou et al., 2022b). Previous studies indicate that temperature and precipitation are two dominant meteorological factors for the Chaohu Lake (Ma et al., 2021). HABs are favored by higher temperatures (25℃-30℃) and light rain, which is why HABs in Chaohu grow fast in hot and wet summers. The wind force is a complicated driving force to the spatial distribution of HABs, as it may gather floating algae or boost the vertical movement of nutrients and aggravate HABs (Zhang et al., 2021; Hu et al., 2021). Sunshine duration is another complicated factor for HABs: appropriate sunshine duration is positively correlated to HABs, while too low sunshine hours may inhibit algae, and too much sunshine may also make algae inactive (Ma et al., 2021; Chen et al., 2021; Jing et al., 2019). Human activities are crucial to HABs, especially inland shallow lakes with low water exchange rates (Qin et al., 2022). Various typical HABs prone lakes are located beside cities or industries, such as Taihu Lake, Dianchi Lake, and Dongting Lake. Negative human activity factors on algal blooms include pollutant inflow, population, economic growth, etc. (Zhao et al., 2019; Khalil et al., 2022), while positive factors include pollutant controlling measures, ecological restoration, biological measures, etc (Box et al., 2021). Driving forces of these factors were analyzed using both quantitative and qualitative methods, such as correlation coefficients, multiple regression, time series analysis and qualitative comparisons (Xia et al., 2019; Busico et al., 2020).

Despite analysis of driving forces, the development of HABs remains a complicated issue as the driving forces vary significantly between different areas and periods. For instance, Guo et al. (2022) compared the similarities and differences between Chaohu Lake and Taihu lake, as both are large inland lakes with similar HABs situations, meteorological conditions, and social development. They found that the temporal trend of HABs in Chaohu Lake varied more than in Taihu lake from 2000 to 2019. HABs in both lakes expanded from lakeside to lake center since 2015, and total phosphorus played a more critical role in both lakes after 2008. However, there remains some uncertainty on the impact of certain factors, i.e., how and how much the inflow nutrients aggravated HABs in Chaohu Lake, as the long-term historical water quality data varied greatly due to social development level and water management measures.

Satellite remote sensing products differ in their parameters for observation start year, spatial resolution, temporal resolution, return period and band ranges, etc. Generally, there exist trade-offs among remote sensing products because no product has the best performance in all features (Gholizadeh et al., 2016). For instance, MODIS remote sensing has significant advantages and disadvantages in observing HABs (Xiong and Barnes, 2006): it has high temporal resolution and sufficient spectral bands but low spatial resolution and frequent missed data caused by cloud cover. Although various satellite remote sensing products have been adopted in HABs observation, few studies discuss the applicability of specific satellite remote sensing products in observing HABs in detail, addressing an exciting topic to judge whether the MODIS satellite is a good choice in HABs analysis.

This study analyzed HABs in Chaohu Lake using MODIS remote sensing daily observations from 2000 to 2021. Detailed analysis of spatial and temporal dynamics of HABs over the past two decades was derived. Potential driving forces, including precipitation, temperature, wind speed/direction, socioeconomic development, and water management policies, were analyzed to indicate their correlations with HABs in Chaohu Lake. Lastly, MODIS remote sensing products' applicability and potential advantage in highly dynamic HABs observations and management were illustrated.

The overall framework of this study is shown in Fig. 1. The rest of this paper is organized by the following framework: The data and its processing method are introduced in Section 2; spatio-temporal dynamics results are presented in Section 3; driving forces to HABs variations as well as the advantage of MODIS product of this study are discussed in section 4.

2. Material and methods

2.1. Study site

Chaohu Lake (117° 16′54″-117°51′46″E,31° 43′28″-31° 25′28 " N), a classically eutrophic lake in China, was employed as the study site in this paper. It is China's fifth largest shallow inland lake, with an average depth of 2.67 m and an average water level of 8.37 m above sea level. Fig. 2 shows the location of Chaohu Lake. Among the ten main tributaries of the numerous tributaries of Chaohu Lake, nine are inflow tributaries, which facilitate nutrients in the basin flowing into the lake. The unique outflow tributary is the Yuxi river at the east lakeside.

The meteorological factor and socioeconomic conditions create favorable conditions for HABs outbreak in Chaohu Lake. Firstly, Chaohu Lake lies in China's warm and wet subtropical monsoon region, with an average annual temperature of 15.8℃ and average annual precipitation of 1000 mm. 60 % to 70 % of the precipitation concentrates in summer (May-October). The synchronous hot-humid climate is very suitable for algal bloom outbreaks. Secondly, the rapid development of urban agglomeration in the basin since the 1980 s, especially the Hefei city to the northwest lake. As the capital of Anhui province, the scale and economy of Hefei city have grown rapidly during the past two decades. Thus, continuous nutrient loadings flowed into the Chaohu Lake through tributaries, resulting in HABs in Lake Chaohu. HABs have occurred almost every year since the 1990s, and the severity is increasing. In summary, the algal blooms of Chaohu Lake are characterized by high frequency, high temporal variance, and high spatial diversity.

2.2. Data

2.2.1. MODIS observations data

MODIS satellite, launched in 1999, is a large space remote sensing instrument developed by NASA. The MODIS surface reflectance products estimate the surface spectral reflectance with 36 bands every 1–2 days. In this study, two MOD09 products, MOD09GQ and MOD09GA, were used as a database for extracting algal blooms of Chaohu Lake. The detailed specifications of the MOD09 product are referred to in https://lpdaac.usgs.gov/documents/306/MOD09_User_Guide_V6.pdf. Table 1 presents main parameters of the two products.

A total of 7926 images were acquired from the MOD09 database, forming a continuous observation of the Chaohu Lake. Table 2 lists the number of images for each year. The severity and coverage of HABs in

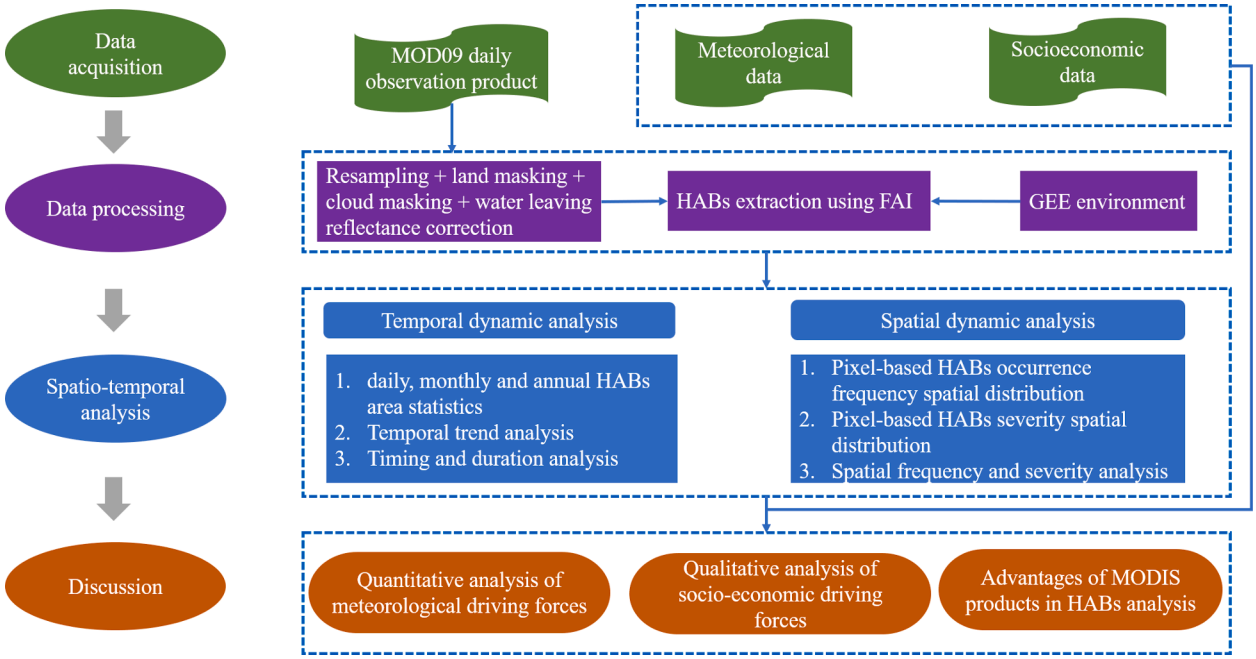

Fig. 1. Framework of paper.

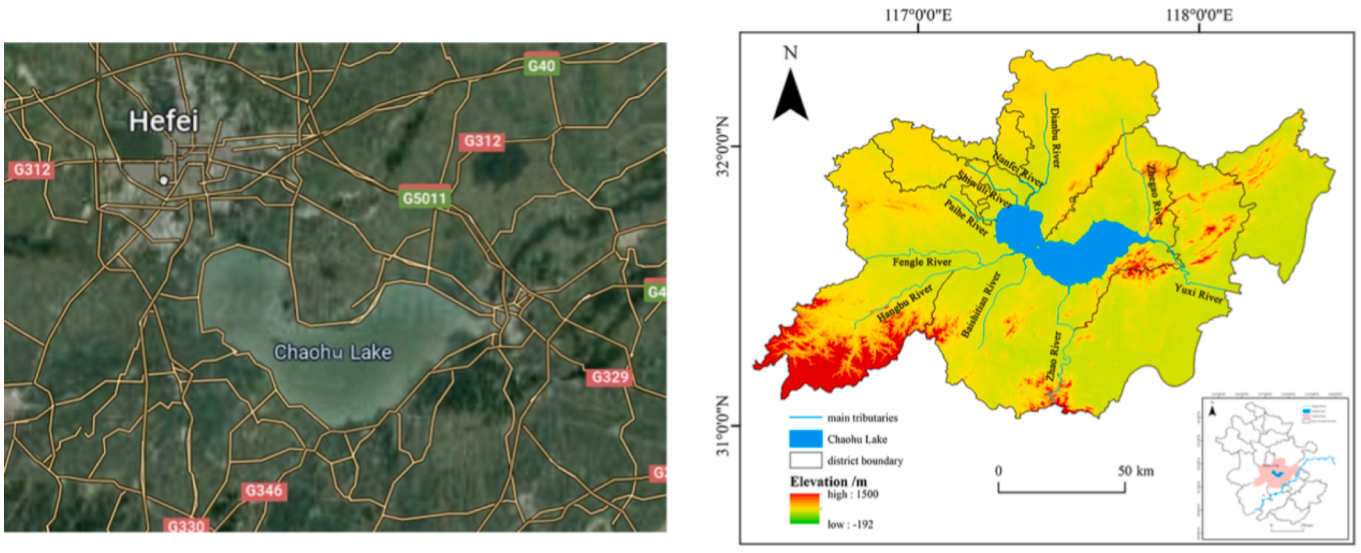

Fig. 2. Location of Chaohu Lake.

Table 1
Main parameters of MOD09GQ and MOD09GA.

Product	Revisit	Parameters			
		Name	Spatial Resolution (m)	Wavelength (nm)	Description
MOD09GQ	Daily	b01	250	620–670	red band
		b02	250	841–876	near-IR (NIR) band
MOD09GA	Daily	b05	500	1230–1250	SWIR1 band
		b06	500	1628–1652	SWIR2 band
		b07	500	2105–2055	SWIR3 band

this paper were derived from each image to reveal the algal bloom's spatial and temporal evolution pattern during the past two decades.

2.2.2. *Driving forces data*

Although a generally recognized driving force set has not been established, the most often considered driving forces can be categorized into meteorological and human activity factors. In this study, these two types of driving forces are also evaluated based on data availability.

1. Meteorological driving forces. Meteorological data of Chaohu Lake were obtained from the Integrated Surface Data – Lite, announced by NCDC (National Climatic Data Center) of NOAA, USA. The dataset covers numerous stations worldwide, and for Chaohu Lake, we use station No. 58321. The scale of data is an hour. Meteorological records, including temperature, wind speed, cloud cover, and precipitation, were utilized in this paper.

2. Human activity driving forces. Considering data availability, GDP,

Table 2
Numbers of images for each year.

Year	2000	2001	2002	2003	2004	2005	2006	2007	2008	2009	2010
Image amount	312	365	365	365	366	365	365	365	366	365	365
Year	2011	2012	2013	2014	2015	2016	2017	2018	2019	2020	2021
Image amount	365	366	365	365	364	367	365	365	362	369	309

population of the neighboring city Hefei of Chaohu Lake, and water management policies were considered in human activity driving forces. The population and GDP of Hefei city were obtained from the government's yearbook. We have been keeping abreast of the water management policies for the past ten years. The water management policies and related water condition data referred to in this paper are cited from official government portals.

2.2.3. Data pre-processing and GEE platform

The MOD09 database is L2 remote sensing product, which was previously corrected for atmospheric conditions such as gases, aerosols and Rayleigh scattering. In this study, the pre-processing of MOD09 refers to resampling, land masking, cloud masking, and water-leaving reflectance correction (Jia et al., 2019). First, the MOD09GQ was resampled to 250 m using bilinear interpolation to implement a better spatial resolution. Land surface and cloud pixels often have similar spectral features with HABs, so they should be masked to avoid signal interference, called land masking and cloud masking. To obtain a more stable reflectance performance of inland water areas, water-leaving reflectance corrections were carried out using the simple but effective method proposed by Wang et al. (2016). After these pre-processing, the images were considered calibrated and appropriate for HABs detection.

Processing 7926 remote sensing images using traditional one-by-one processing manners is unrealistic. Several cloud computing platforms have been developed to address this issue, and one of the most widely used platforms is Google Earth Engine (GEE) (Alikas et al., 2010; Song et al., 2022). GEE is a cloud-based geospatial processing platform for large-scale environmental monitoring and analysis. Till now, the GEE platform has provided research support in various fields such as vegetation observation (Johansen et al., 2015), water environment monitoring (Lobo et al., 2021), flood monitoring (DeVries et al., 2020), and different geo-big data analysis (Tamiminia et al., 2020).

This study applies GEE as the remote sensing processing platform. The GEE platform significantly improved data processing efficiency and provided an essential guarantee for data acquisition and analysis of the vast information load.

2.3. HABs detection indicator

When cyanobacteria proliferate and distribute on large water surfaces, the spectral characteristics of the water surface are similar to vegetation, so indicators detecting vegetation can be adapted to detect algal bloom in water areas. The FAI indicator, proposed by Hu (2009), is a specific indicator to detect algae in the water. FAI is an ideal indicator to identify HABs in lakes and oceans as it is less sensitive to environmental interferences such as cloud cover, aerosol thickness, and solar scintillation than NDVI and EVI. In this study, the FAI indicator is derived from The MODIS Surface Reflectance product. The product provides an estimate of the surface spectral reflectance as it would be measured at ground level in the absence of atmospheric scattering or absorption.

The original description of FAI is as follows:

$$FAI = R_{rc,NIR} - R'_{rc,NIR} \tag{1}$$

$$R'_{rc,NIR} = R_{rc,RED} + \left(R_{rc,SWIR} - R_{rc,RED}\right) \bullet \frac{\lambda_{NIR} - \lambda_{RED}}{\lambda_{SWIR} - \lambda_{RED}} \tag{2}$$

where $R_{rc,NIR}, R_{rc,RED}, R_{rc,SWIR}$ are Rayleigh corrected red reflectance, near infrared reflectance and short infrared reflectance, λ_{RED} is the infrared center wavelength, λ_{NIR} is near infrared center wavelength, and λ_{SWIR} is short wave infrared center wavelength.

In this study, as the MOD09 surface reflectance product is used, $R_{rc,NIR}, R_{rc,RED}$ and $R_{rc,SWIR}$ correspond to corrected reflectance $R^c_{rs,NIR}$, $R^c_{rs,RED}$ and $R^c_{rs,SWIR}$, respectively (Jia et al., 2019). The corrected reflectance of MOD09 product centered at wavelength λ,$R^c_{rs}(\lambda)$, is derived by:

$$R^c_{rs}(\lambda) = \frac{R(\lambda) - \min(R_{NIR} : R_{SWIR})}{\pi} \tag{3}$$

where $R(\lambda)$ is the original MOD09 reflectance at wavelength λ, $\min(R_{NIR} : R_{SWIR})$ is the minimum positive reflectance value between NIR and SWIR bands, and π is the denominator to transform surface reflectance to reflectance.

Zhang et al. (2015) calibrated the threshold of HABs for Chaohu Lake, which is −0.0026 of the FAI indicator. We have tested the reasonability of this threshold by comparing the derived HABs area with the "ground true" area announced by the Department of Ecology and Environment of Anhui Province. The official severity of HABs were published online: https://sthjt.ah.gov.cn/public/21691/110831651.html. The derived HABs area using threshold −0.0026 fits the official announcement well. Therefore, in this study, we distinguish HABs and non-HABs areas using a threshold of −0.0026; that is, pixels with FAI value greater than −0.0026 is regarded as algae coverage, otherwise, it is considered as a non-algae area.

2.4. Spatio-temporal dynamics analysis of HABs

Spatial and temporal dynamics analysis was carried out by calculating FAI values for each pixel. Fig. 3 illustrates the general idea of temporal and spatial analysis. Details of the spatial and temporal analysis is explained in 2.4.1 and 2.4.2.

2.4.1. Temporal dynamics

1. Daily, monthly, and annual HABs area statistics. A binary classification of FAI was applied to all pixels of each MODIS observation between 2000 and 2021. Knowing that each pixel covers a 250 m*250 m area in MODIS images, algae coverage was converted from HABs pixel numbers multiplied by the area of the pixel unit. Based on daily HABs coverage, monthly average and annual average HABs coverage were further inferred by averaging daily HABs area time series data.

2. Temporal outbreak frequency. Each year's temporal frequency of a large area HABs outbreak is a key symbol for assessing the severity of algal blooms. This study divides HABs outbreaks into three grades: light, medium, and heavy. According to the announcement of the Department of Ecology and Environment of Anhui Province, algal blooms were divided into "scattered little", "light", "medium" and "heavy" grades. Both HABs area and distribution determined the grades. Based on the long-term announcement, we defined in this paper that light grade refers to HABs coverage between 100 km^2 to 200 km^2 (15 % − 30 % of the lake area); medium grade refers to HABs coverage between 200 km^2 to 300 km^2 (30 % − 45 % of the lake area), and heavy grade HABs coverage greater than 300 km^2 (greater than 45 % of the lake area). The outbreak times of each year were counted to reveal HABs frequency and severity.

3. Monthly average HABs area. Since HABs are highly sensitive to temperature and have seasonal periodicity, monthly average HABs areas

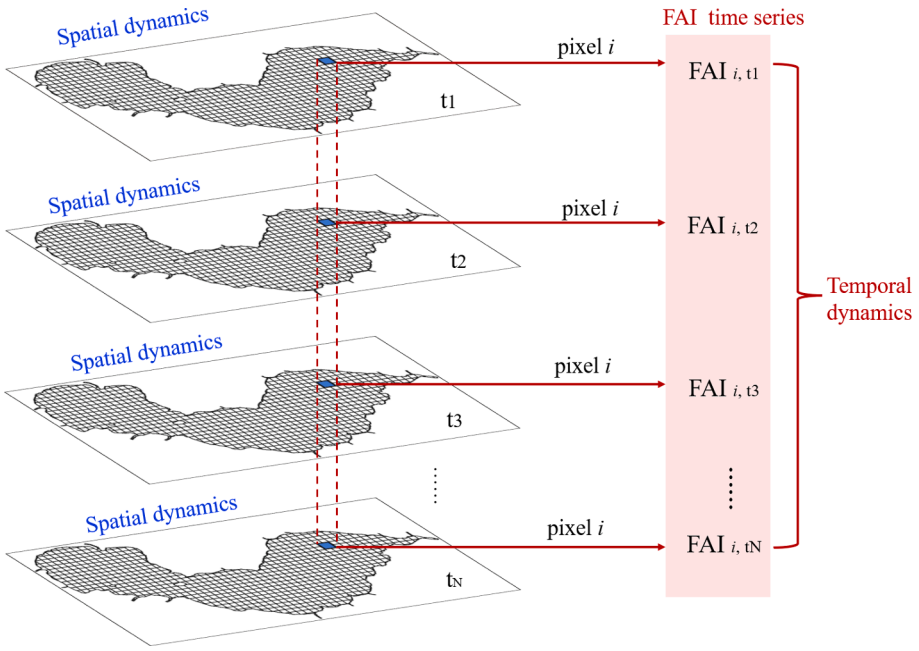

Fig. 3. Sketch of temporal and spatial analysis.

are derived to illustrate the seasonal evolutionary pattern. The monthly average HABs area is derived by averaging the HABs area of all images of each month from 2000 to 2021.

4. Maximum HABs area. HABs distribution is highly dynamic in both temporal and spatial dimensions due to its fast-growing feature and sensitivity to meteorological factors; moreover, algal bloom distributions observed from remote sensing images are often masked by cloud cover, which may underestimate algal bloom coverage. Therefore, the maximum HABs areas observed from remote sensing images are more representative in reflecting algal bloom peak situations. Here, the maximum HABs area for each year was selected and presented. Furthermore, the occurrence month of the maximum HABs area was also given to illustrate the timing of the most severe HABs.

5. Start time, end time, and duration of HABs. Taking HABs coverage greater than 100 km^2 as the threshold of HABs outbreak, start time, end time, and duration can be derived from the daily HABs area time series. The first date that HABs area exceeds 100 km^2 was regarded as the year's start time; similarly, the last date that HABs area exceeds 100 km^2 was regarded as the year's end time, and the time between start time and end time was taken as duration of HABs in a year.

2.4.2. Spatial dynamics

HABs in Chaohu Lake are more uneven in spatial distribution due to the low flow speed and various onshore influences. To analyze the spatial dynamics of HABs and their evolutional pattern over time, spatial frequency and severity were derived.

1. Spatial frequency. The spatial frequency of HABs refers to the occurrence times of HABs for each pixel during a year, as illustrated in Fig. 3. The spatial frequency map of the overall lake can be drawn based on the frequency of each pixel.

2. Spatial severity. Maximum FAI analyzes the spatial severity of HABs for each pixel during a specific period. To reduce the influence of missing pixel FAI values due to cloud cover, we adopt maximum FAI to describe the spatial severity instead of the average value (Zhou et al., 2022a). We did not remove the "imperfect" images with partially missing data caused by cloud cover, because preserving as much useful information as possible could help reveal the trend of the high dynamics of HABs.

In conclusion, the spatial dynamics are derived by overlapping all images during a specific year and derived from values in each pixel. From spatial dynamic analysis, the general distribution of multiple HABs spatial distributions can be summarized and presented.

3. Results

3.1. Temporal variations analysis

Fig. 4 presents daily HABs coverage from MODIS observation based on 7926 MODIS images. The blue curve refers to the daily HABs area, and the red curve is the maximum area of each month. To illustrate the general trend of HABs area variations, the monthly average area series is calculated and presented, shown in Fig. 5.

It can be indicated from Fig. 4 and Fig. 5 that despite the HABs area varying greatly from year to year, there exist significant cycles. That is, HABs area reaches a peak in summer (July to September) and shrinks in winter, which is quite accordant with temperature. HABs are basically stable and light before 2010 and gradually increase after 2010. The daily HABs area in Fig. 4 clearly demonstrates that since 2012, HABs occurrences have become more frequent, and the peaks often occurred more than once a year, often emerging several rounds of HABs growing cycles. Severe and frequent HABs were noticed in 2014, 2015, 2018 and 2019.

To compare daily HABs area regimes of each year, Fig. 6 presents the boxplot of HABs area for each year. Since HABs area on most days was quite low, the natural logarithm axis was used to distinguish the quantiles better. The boxplot shows that the upper and lower limits vary greatly from year to year, indicating that the HABs severity and frequency vary greatly. The median value is a more subject indicator of HABs severity than the maximum or average values, as it represents the overall level of all HABs data within a year. For instance, HABs in 2019 have the highest median value, indicating that HABs in 2019 are one of the severest among all years, although their maximum value is lower. This inference agrees with the following results.

Each year's HABs outbreak frequency was counted and shown in Fig. 7. The average occurrence frequency of HABs outbreaks is 38 days a year, while the frequency varied greatly and showed dramatic time-varying trends. The average outbreak frequency from 2000 to 2006 was 26 days, then increased to 39 days from 2007 to 2017, and sharply increased to 75 days in 2018 and 2019, followed by a sharp decrease to 37 days in 2020 and 2021. The year with the highest HABs frequency was 2019, whose HABs occurrences reached 87 days, and heavy HABs

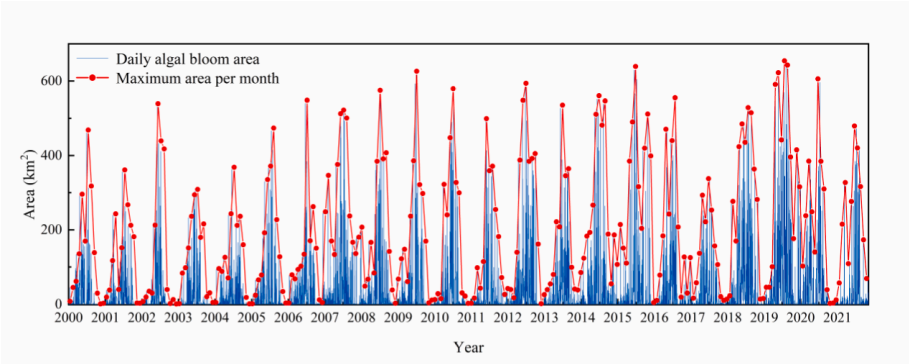

Fig. 4. Variation of the daily area of algal blooms in Chaohu Lake from 2000 to 2021倪程:此图增加分辨率.

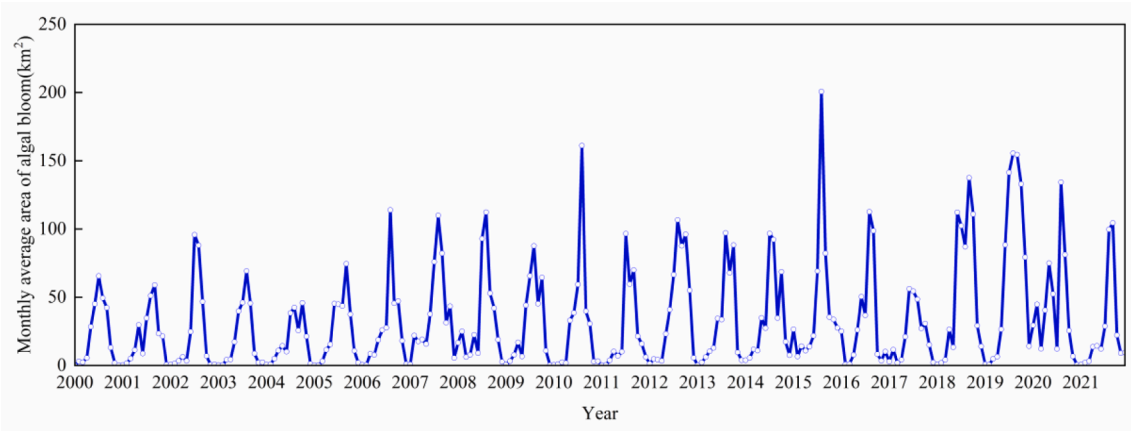

Fig. 5. The monthly average area of algal blooms from 2000 to 2021.

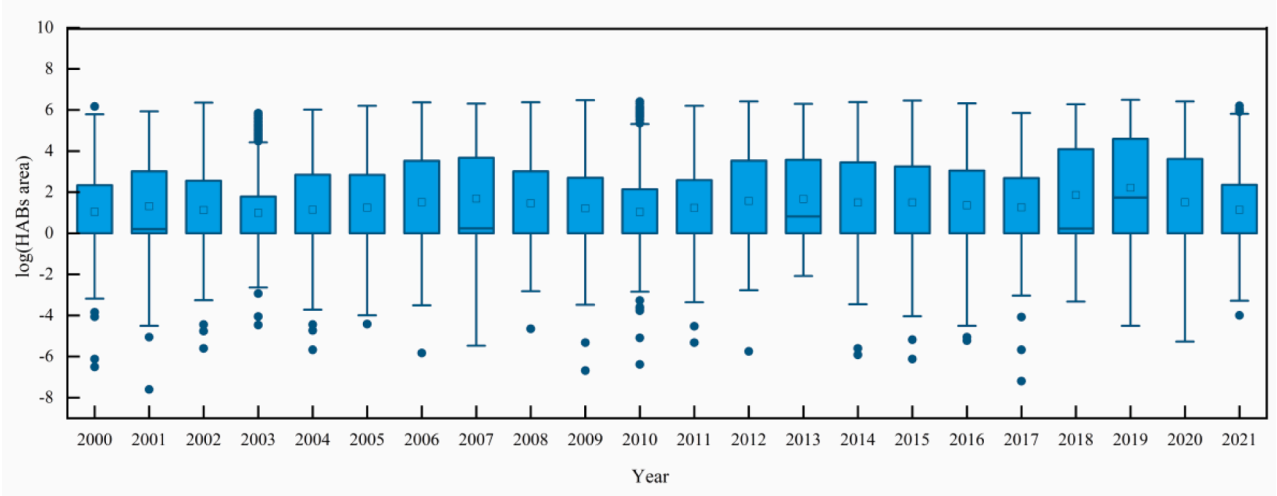

Fig. 6. The annual average area of algal blooms from 2000 to 2021.

occurrences reached 26 days. Xue et al. (2022) tracked the dynamics of FAI using MODIS, VIIRS, GOCI, and OLCI images, showing that Lake Chaohu experienced severe algal blooms after 2010 similar with the results in Fig. 7.

Qin et al. (2022) compared the HABs evolutional pattern of Chaohu with that of Taihu, which is also one of the largest inland lakes with severe HABs. It was found that the temporal trend of HABs in Chaohu was more complicated than that in Taihu in the past few decades. Here, based on temporal trends on daily, monthly, and annual scales, the HABs evolution course of Chaohu Lake is divided into four stages:

Stage 1 (2000–2006). In this stage, the HABs area in Chaohu Lake was relatively low and stable, and the frequency of severe algal blooms was relatively rare. The maximum bloom area is 550 km^2.

Stage 2 (2007–2017). The HABs area increased significantly in this stage. The maximum outbreak time occurred in 2015, accounting for 47 times. The maximum bloom area occurred in 2009, reaching 616.52 km^2. The frequency of severe algal blooms increased significantly and became a common phenomenon, indicating that the algal blooms were

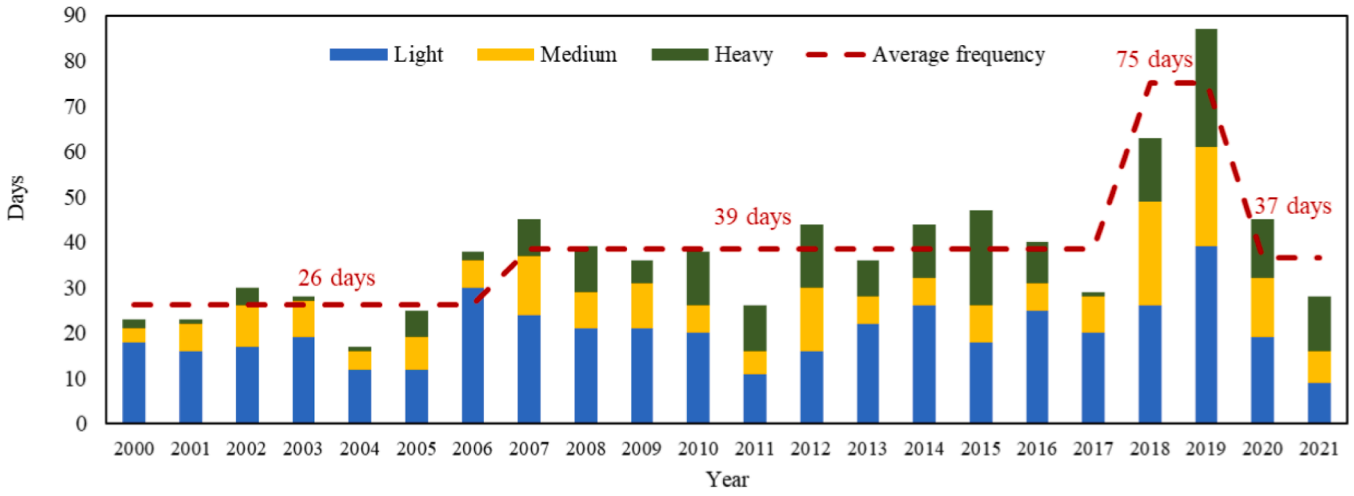

Fig. 7. Frequency of HABs area from 2000 to 2021.

getting more severe. A decrease in HABs area emerged in 2016 and 2017, likely because the average temperature in the summers of the two years was lower than the average value historically, and strict environmental countermeasures were carried out during the two years. This short sudden decrease in HABs was also highlighted in reference (Qin et al.,2022).

Stage 3 (2018–2019). The severity of algal bloom strongly rebounded considerably after 2018, showing a sharp increase in both HABs area and severity. HABs frequency reached its peak in 2019, amounting to 87 times; meanwhile, the average HABs area reached its peak in 2019, amounting to 67.49 km^2. These two years were the severest during all 22 years, severely impacting the environment and human lives.

Stage 4 (2020–2021). The HABs severity suddenly decreased in 2020 and 2021, just after the sudden increase in 2018 and 2019, which posed significant shifts. The frequency of HABs was 45 times and 28 times, respectively. Although there were over ten occurrences of severe HABs, the total occurrences showed a significant decrease since 2019. The sudden improvement was mainly due to powerful water pollutant-controlling countermeasures, which will be discussed in detail in 4.1.2.

Fig. 8 shows the monthly mean HABs area from 2000 to 2021. It is indicated that algal blooms were rare in the winter to the spring season, from December to April. The extent of algal blooms expanded from May, peaked in August, and then slowly decreased. The trend of algal blooms was highly accordant with temperature trends, indicating that temperature is a critical factor in triggering algal blooms. Detailed examination shows a slight delay of HABs area peak (occurred in August) compared with the temperature peak (occurred in July) because of algae's proliferation and accumulative process. These trends are consistent with results from previous studies of Chaohu Lake (Qin et al.,2022).

Fig. 9 presents the maximum area of HABs and their occurrence month for each year. The annual maximum HABs area mainly occurred in August, accounting for 16 years among all 22 years. The maximum extent tended to be lower and stable before 2007; since 2008, the maximum area significantly increased and kept at a high level (except in 2017). The maximum HABs area occurred in 2019, reaching an area of 644 km^2, covering 82 % of the Chaohu Lake. The maximum HABs area tended to increase from 2000 to 2021.

Fig. 10 presents the start and end months of each year. It is indicated that from 2000 to 2006, algal bloom occurrences mainly concentrated in June to October; since 2007, the start time became earlier, and the duration became longer. Algal bloom lasted until December 2015 and started in January 2016, showing an ongoing outbreak throughout two years. Generally, the agal bloom duration has been getting longer in recent 15 years.

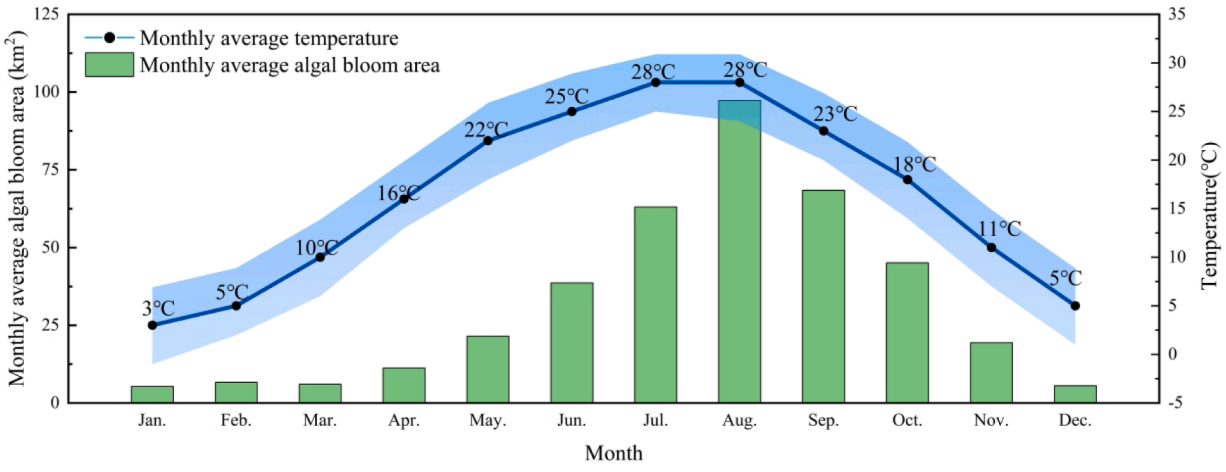

Fig. 8. Monthly average HABs area from 2000 to 2021.

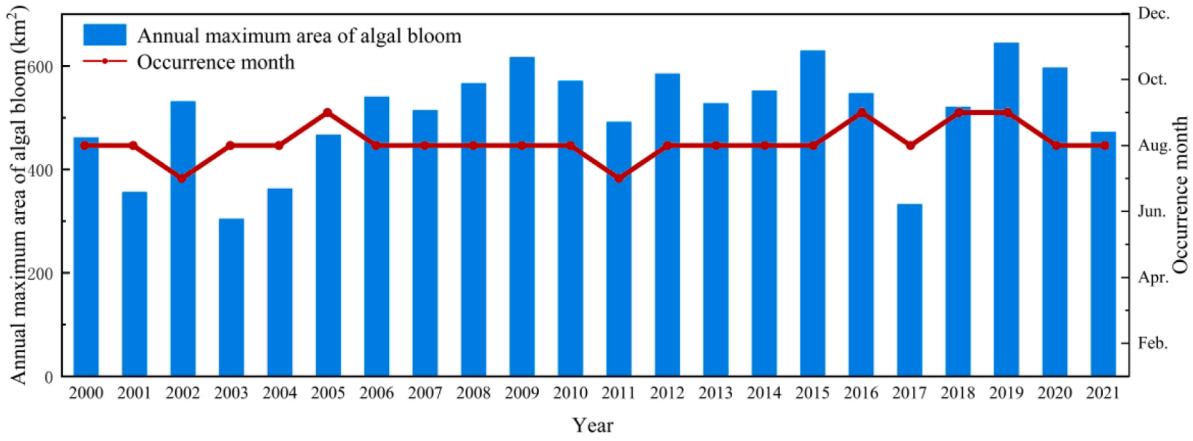

Fig. 9. Annual maximum HABs area and their peak months from 2000 to 2021.

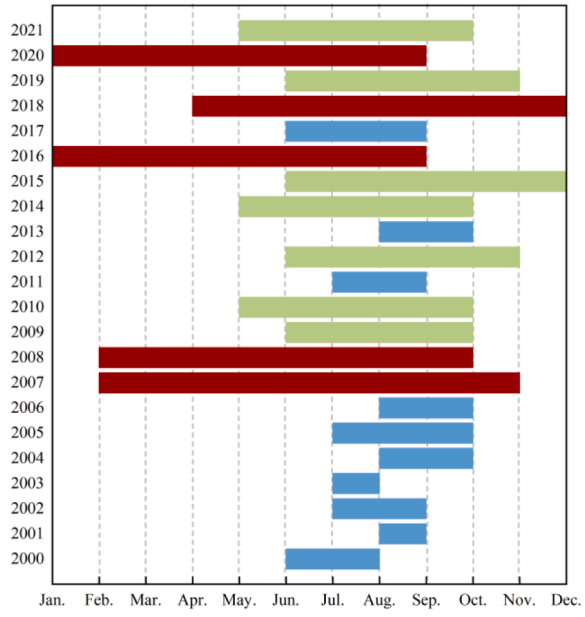

Fig. 10. Start time, end time and duration of HABs in Chaohu Lake from 2000 to 2021 (blue: duration shorter than 3 months; green: duration between 4 and 6 months; red: duration longer than 6 months). (For interpretation of the references to colour in this figure legend, the reader is referred to the web version of this article.)

3.2. Spatial variations analysis

To analyze the spatio-temporal trend of algal bloom evolution during the past two decades, HABs frequency distribution were derived to indicate the distribution of HABs, shown in Fig. 11. Besides, annual average FAI was calculated to indicate the general severity of HABs, shown in Fig. 12.

Fig. 11 and Fig. 12 indicated that HABs concentrated in the northwestern part of the lake for almost all years, both in frequency and severity. This feature is accordant with previous studies (Qin et al.,2022), mainly due to the human activity influences from Hefei city lies to the northwest of Chaohu Lake (Fig. 2). With more than 9 million population, domestic and industrial sewage of Hefei city flows into Chaohu Lake through tributaries. As a result, the eutrophication of the northwestern lake has long been aggravated.

Temporal trends of HABs spatial distribution also revealed the evolution pattern of HABs. From 2000 to 2006, algal blooms were generally light and stable, mainly concentrated in the northwestern lake; from 2007 onwards, agal blooms began to spread from lakeside to the lake center, and the occurrence frequency of the northwestern lake also increased, indicating increasing severity of algal blooms. The frequency of large-scale outbreaks (area greater than 300 km^2) also increased significantly, reaching 23 times in 2015. There was a retracement in 2016 and 2017. However, in 2018, the blooms began to erupt in the whole lake, with the outbreak frequency peaking in 2019. In 2020 and 2021, there is a sharp decrease of HABs severity, which will be discussed in 4.1.2.

4. Discussion

4.1. Driving Forces of HABs

4.1.1. Meteorological driving forces

A previous study analyzed the influence of precipitation and temperature on algal blooms in Chaohu Lake (Coffey et al., 2018). They found significant increasing temperature trends and slight precipitation trends in the lake region. Thus, the deterioration of HABs was preliminarily ascribed to the increase in temperature and precipitation.

As introduced in 2.2.2, daily meteorological data were collected, including precipitation, temperature, cloud cover, wind direction, and wind velocity. Fig. 13 presents monthly average temperature, precipitation, and cloud cover trends.

As Fig. 13 shows, there exist clear correlations between precipitation, temperature, cloud cover, and HABs area. Temperature and HABs area aroused simultaneously from May to October and decreased from November to March, which indicated a clear positive correlation between temperature and HABs. Precipitation varied greatly from season to season. It was difficult to observe its correlation with HABs from the Fig. 13. Coffey et al. (2018) reviewed various driving factors of water quality to document how different water quality attributes are sensitive to these drivers. They concluded that the effects of most factors are complicated, and precipitation is the only factor that positively correlates with water quality "in all regions" likely because heavy precipitation drives more episodic pollutant loading to water bodies. This is different from some intuition that precipitation will improve water quality by diluting pollutants in water body. Cloud coverage is also related to HABs, as it may reduce nutrient utilization by phytoplankton (D'Silva et al., 2012; Patil and Anil, 2008; Cho et al., 2014; Cao et al., 2011). In other words, cloud cover is likely to correlate with HABs

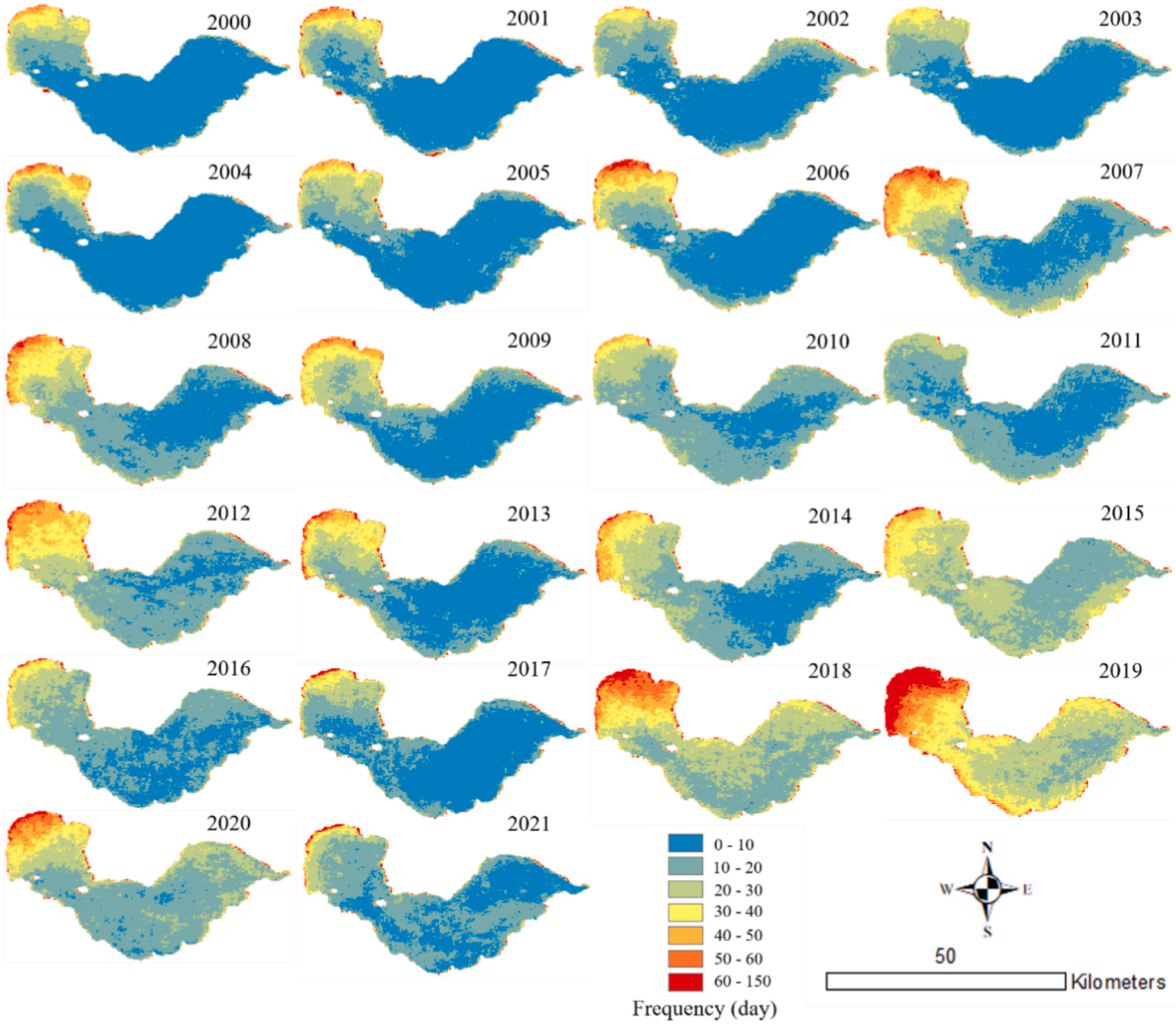

Fig. 11. Spatial distribution of algal bloom occurrence frequency from 2000 to 2021.

negatively.

Table 3 shows the correlation coefficients among the driving forces and HABs. HABs area is highly correlated to temperature, with a coefficient of 0.70. Precipitation is also positively dependent on the HABs area. In contrast, the correlation coefficient between cloud cover and HABs area is much smaller than other variables.

To illustrate the contribution of temperature and precipitation to HABs area, a linear regression equation using monthly indicators was found as follows:

$$S = -17.80 + 2.49T + 0.09P \quad (2)$$

Where S is the monthly average HABs area of Chaohu Lake in km^2, T is the monthly average temperature in ℃, P is the monthly total precipitation in mm. The multiple regression analysis yields an R^2 coefficient of 0.52, indicating that 52 % of the variation in HABs area can be explained by temperature and precipitation, as other types of driving forces influence algal blooms, such as wind conditions, urbanization, and water management policies.

The regression equation reveals that precipitation and temperature positively correlate to HABs area. With increased precipitation or temperature, HABs area is likely to increase. This explains why the HABs area expands rapidly in hot and wet summers. Fitting performance shows that the regression equation better predicts low and medium HABs areas than high to peak HABs. The reason is that the algal bloom area may increase rapidly in a short time triggered by short and intensive environmental variables. However, monthly climate variables are typically smoother, so the regression equation will likely underestimate peak HABs areas.

The wind force is another crucial factor that may influence the distribution of algal blooms. A previous study suggested that the HABs area in Taihu lake significantly decreases when wind speed exceeds 4 m/s because of the turbulence and changes in algal buoyancy caused by wind force (Huang et al., 2014). Also, Marshall et al. (2015) revealed a negative correlation between wind intensity and algal blooms.

The wind force is a vector characterized by both intensity and direction. Chaohu Lake lies in the monsoon climate zone with distinctive climate features, so wind direction varies significantly over seasons. This study collected the hourly wind direction and wind speed of the algal bloom season (May to October) from 2000 to 2021 from NCDC introduced in 2.2.2. Fig. 14 presents the wind rose map with the frequency and intensity of wind forces each month. The rose map shows apparent shifts in wind direction over months, from south and east direction to north and east directions. Generally, the east and south directions are the dominant wind directions in the algal bloom season. On the one hand, wind forces may increase algae's vertical movement, thus decreasing its appearance. This explains why the algae blooms may be quite diverse in very short hours and under constant environmental variables. It was recorded occasionally that the spatial distribution of algal blooms in Chaohu Lake considerably changed in one night because the wind shifted in the opposite direction. On the other hand, algae may

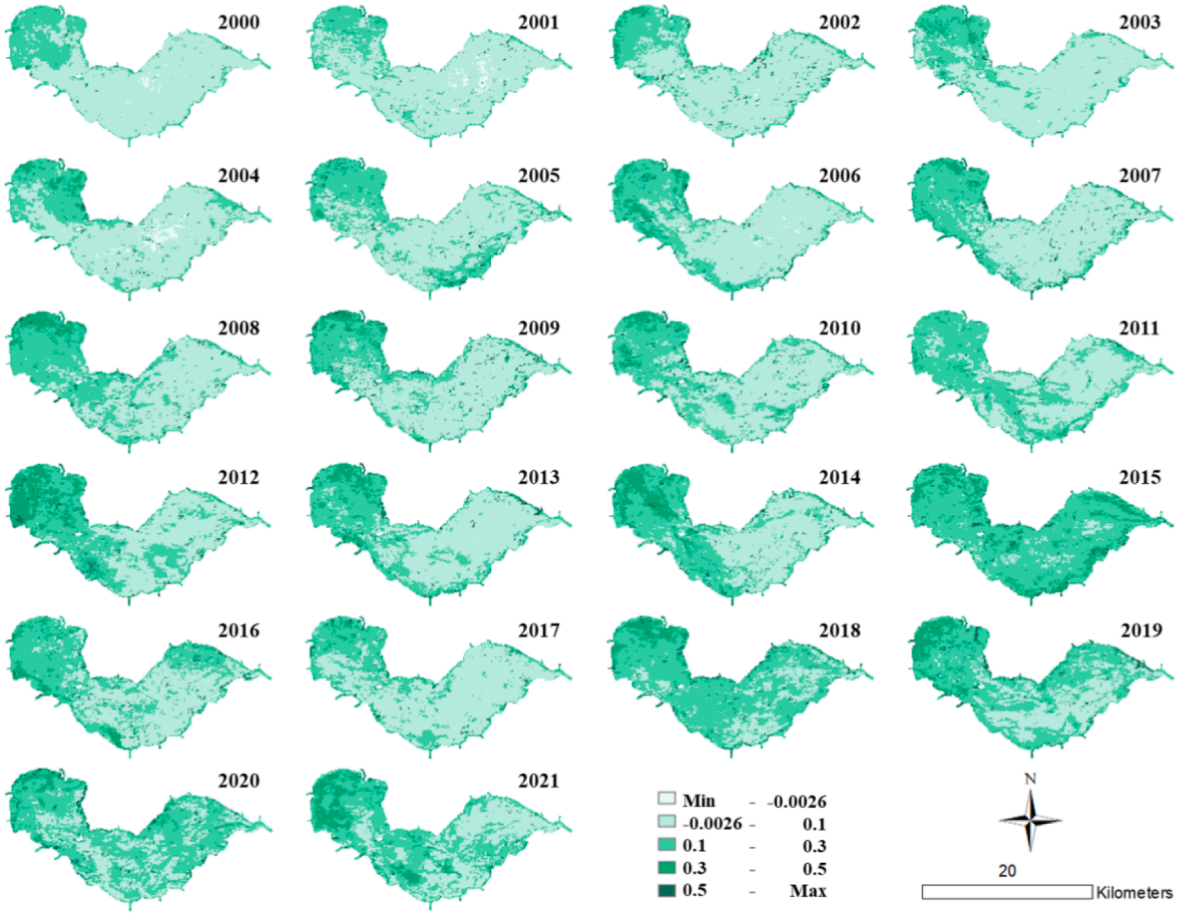

Fig. 12. Spatial distribution of annual maximum FAI from 2000 to 2021.

be gathered in the opposite direction of wind force. This partly explains why the algal blooms in the lake's northern part are much more severe than in the southern part from May to July (Figs. 11 and 13).

4.1.2. Human activity driving forces

Human activities include various elements such as management measures, nutrient inflows, land use, and industrial disposals (Khalil et al., 2022; Abbas et al., 2022). Chaohu Lake has a giant neighboring city: Hefei city. Two main tributaries of Chaohu Lake, Shiwuli and Nanfei rivers flow through Hefei city to the lake. Therefore, it has been a widely accepted view that the economic development of Hefei city has been the most human activity factor for the HABs in Chaohu Lake (Duan et al., 2015). In this study, considering data availability, two main socioeconomic variables, the population and GDP of Hefei city, were collected to reveal its impact on HABs in Chaohu Lake.

Fig. 15 shows the annual population and GDP from 2000 to 2021. The population and GDP increased slowly before 2009 but rapidly since 2010 and have maintained at high speed since then. By comparing the population and GDP trends with HABs trends, it can be indicated that their fast-growing stages were almost synchronized. The fast-growing population and GDP implied fast-growing domestic sewage and industrial wastewater discharge to the Chaohu Lake through its northwestern tributaries, such as Shiwuli, Pai, and Nanfeihe rivers (Fig. 2). Although long-term water quality information is lacking, it was reported that the water quality of these three rivers was the worst among all the tributaries of Chaohu Lake. Numerous inflow nutrients increased the overall eutrophication level of Chaohu Lake, especially the northwestern part of the lake. This explains why the HABs sharply increased after 2008 and why the northwest part of the lake always had the heaviest HABs. Liu et al. (2022) discussed the relationship between microplastics and algal bloom distribution in Chaohu Lake. As a symbol indicator of human activity, it was found that the abundance of microplastics in the estuaries and the western part of the lake were higher than those in other locations, and microplastics could promote the growth of algae blooms in the early stage. This proved the role of human activity in promoting algal blooms and explained the uneven distribution of HABs over the years.

Except for GDP and population indicators, water environment management policy also profoundly influences the algal bloom regime. Since the water environment of Chaohu Lake has greatly threatened the ecology, water supply and human health, the eutrophication and frequent outbreak have addressed much attention from the government except for pursuing economic flourish. In recent years, continuous countermeasures greatly relieved the water environment and HABs in Chaohu Lake. For instance, an inspection of ecological and environmental protection by the Chinese government policed the Chaohu Lake water environment and land use conditions in 2016. It announced strictly that there were infractions in pollutant discharge in 2017. In 2020, Chaohu Lake encountered the highest precipitation, which triggered severe HABs after the storm season. After that, the government carried out the "promote Chaohu Lake as the best name card of Hefei city" Act to systematically curb both the water and basin environment of Chaohu Lake. Ten wetlands around Chaohu Lake, with a total area of 100 km^2, were established (https://www.hefei.gov.cn/english/LocalNews/107972479.html). It should be noted that these powerful environmental management measures require solid financial support. Therefore, the 20-year fast-growing GDP of Hefei city provides a strong guarantee for the measures. From this point of view, GDP is like a double-edge sword that may deteriorate and improve water conditions.

The effect of policy is directly revealed by water conditions before

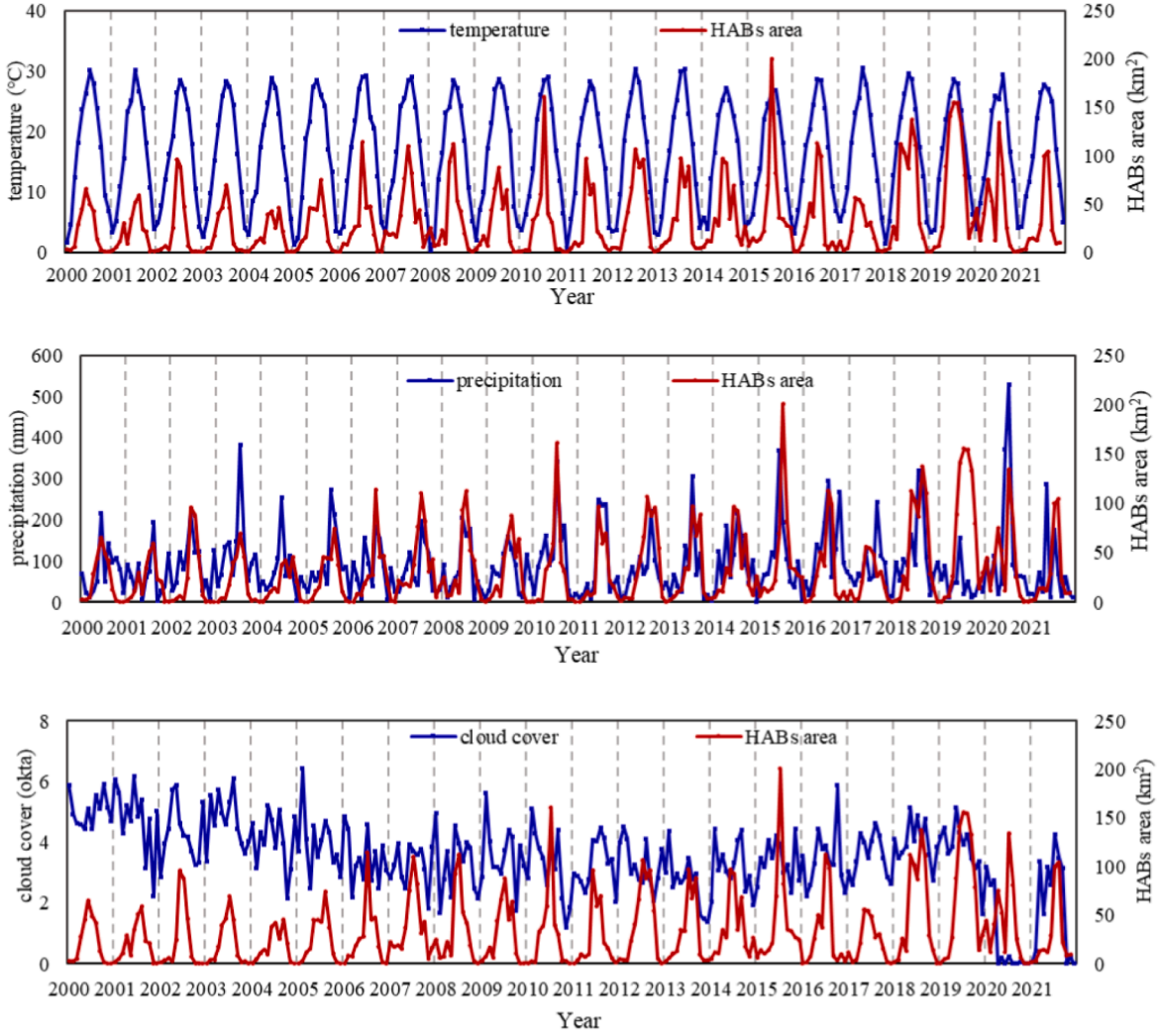

Fig. 13. Temperature, air pressure, cloud cover, and precipitation from 2000 to 2021 in Chaohu region.

Table 3
Correlation coefficients among temperature, precipitation, cloud cover, and HABs area from 2000 to 2021.

	Temperature	Precipitation	Cloud coverage	HABs area
Temperature (℃)	1			
Precipitation (mm)	0.49	1		
Cloud coverage (okta)	0.09	0.21	1	
HABs area (km^2)	0.70	0.49	0.10	1

and after 2020. We collected the main water pollutant indicators including NH3-N, COD and TP in 2019, 2020 and 2021 from local government, shown in Table 4. To better reveal the annual changes, year-over-year variance percentage of each indicator is calculated and shown in Fig. 16.

Firstly, it can be found from Table 4 that the west lake did have higher NH3-N, COD, and TP than the east lake, which is in line with the HABs distribution in previous results. We can see a significant decrease in nutrients since 2020, i.e., NH3-N decreased by over 50 % in 2020 and 2021, and COD decreased by over 10 % in 2021. This reveals that the inflow of eutrophic substances was sharply reduced in the two years. TP, on the contrary, kept stable during the three years. This is because the Chaohu Lake deposited a large amount of phosphorus (Liu et al., 2012), which is unlikely to decrease in a short time.

In general, the water condition of Chaohu lake has significantly improved since 2020, which explains the sudden improvement of HABs. The significant efficiency in policies and countermeasures further reveals that except for meteorological factors, pollutants from human activities are an essential source of HABs. Human countermeasures significantly contribute to HABs decrease. These conclusions align with previous studies (Guo et al., 2022) that various countermeasures have significantly improved HABs in Chaohu Lake since 2020. Similarly, the effect of countermeasures in recent years in another inland eutrophic lake in China, Dianchi, was validated (Ma et al. 2022). The analysis revealed that environmental management measures taken by local governments led to improvements in the lake's trophic state, and continued strengthening of environmental pollution control is expected to curb the algal blooms in Lake Dianchi.

4.2. *Advantages of MODIS remote sensing in HABs monitoring*

Various satellite remote sensing products have been utilized to observe algal blooms, each with advantages and limitations (Marshall and Thenkabail, 2015). For instance, when we choose the Landsat satellite instead of MODIS satellite, we obtain better spatial resolution but give up the better temporal resolution, as the spatial resolution of Landsat and MODIS satellites are 30 m and 250 m, respectively; however, the temporal resolution of Landsat and MODIS satellites is 16-day

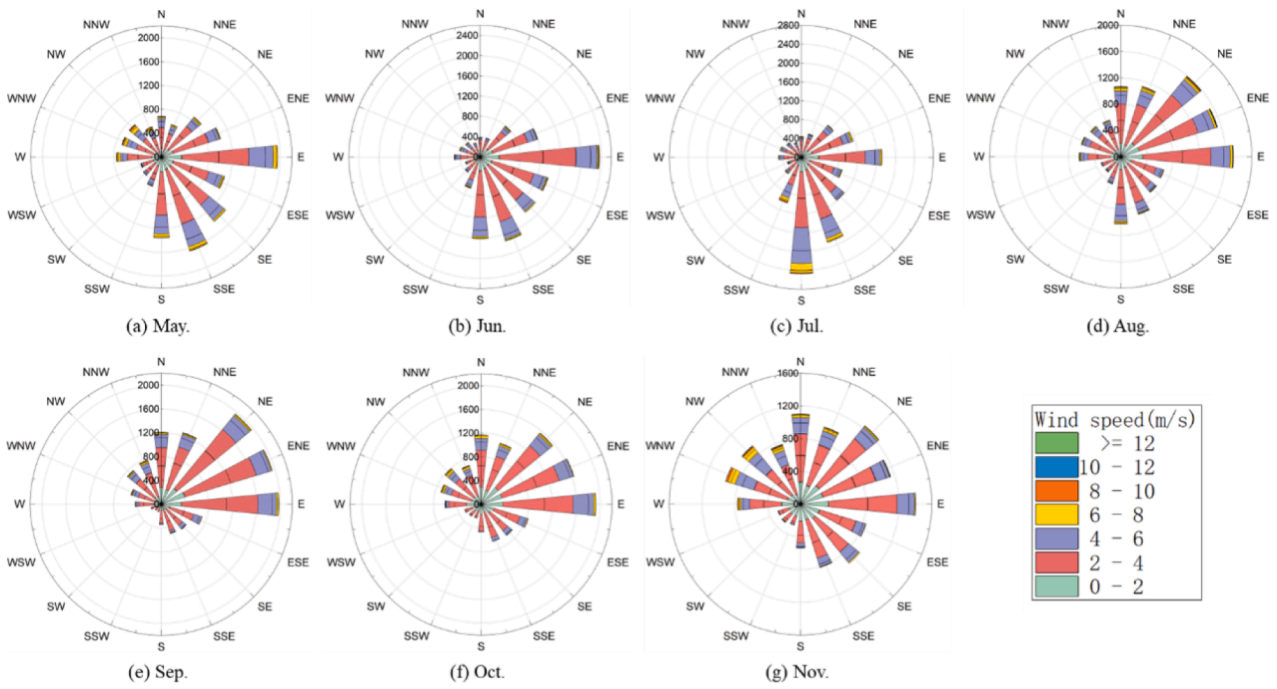

Fig. 14. Wind rose map of each month in HABs season.

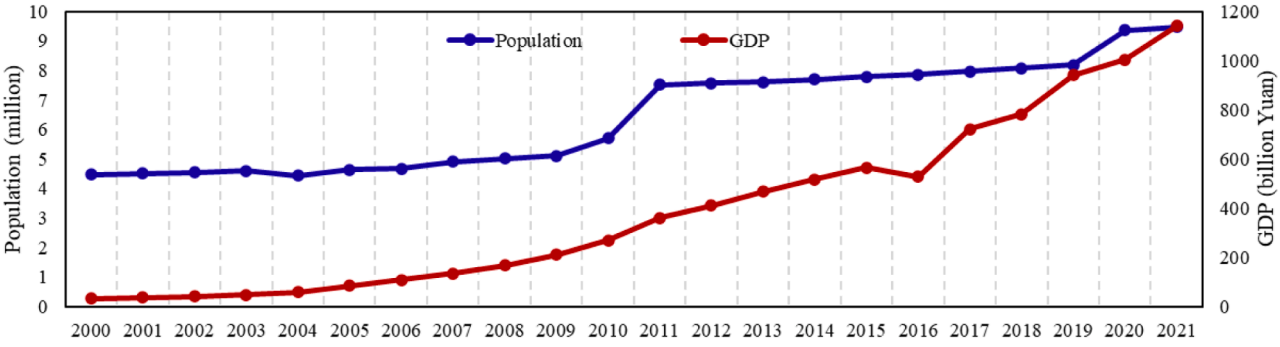

Fig. 15. Annual population and GDP of Hefei city from 2000 to 2021.

Table 4
Annual average NH3–N, COD and TP of Chaohu Lake in 2019, 2020 and 2021 (unit: mg/L).

	Year	NH3–N	COD	TP
East lake	2019	0.12	13.38	0.06
	2020	0.08	14.28	0.06
	2021	0.04	12.11	0.08
West lake	2019	0.25	15.25	0.10
	2020	0.14	14.05	0.08
	2021	0.06	12.58	0.10
Total lake	2019	0.17	14.08	0.08
	2020	0.12	14.14	0.07
	2021	0.05	12.23	0.08

and 1 day. Similarly, suppose we choose the Sentinel satellite instead of the Landsat satellite. In that case, we could obtain better temporal resolution but give up a long-term record, as the Landsat satellite was launched in the 1980 s while the Sentinel satellite was launched in 2014. Many studies noticed the complementary among satellites, so they adopted multiple-source remote sensing data to acquire better performance (Dong et al., 2019; Mu et al., 2019; Zhang et al., 2020). However, blending different satellites involves another critical problem: spectral data calibration and fusion, as different satellites vary in sensors and spectral bands.

The current study reveals the merit of the advantages of MODIS remote sensing in HABs observation. The primary superiority of the MODIS product is the high-frequency observations. As HABs are highly dynamic in spatial and temporal dimensions, the frequency of observations plays an essential role in capturing the variations. With MODIS observations, daily observations can be obtained so that the daily, monthly and annual variations can be derived for detailed spatio-temporal analysis. Although MODIS remote sensing has been criticized for its frequent cloud blockage (Zhao and Duan, 2020; Li et al., 2019), our study proved that as long as the observations are frequent enough, even incomplete images blocked by clouds can "piece together" quite accurate spatial and temporal trends. On the contrary, even with high spatial resolution and cloud-free quality, single images cannot capture the detailed dynamics of HABs. Another advantage of the MODIS product is the complementary spectral coverage and bands. The MODIS remote sensing products provide 36 bands ranging from 0.4um-14.4um, providing high flexibility and capability for advanced band-based calculations such as machine learning and deep learning.

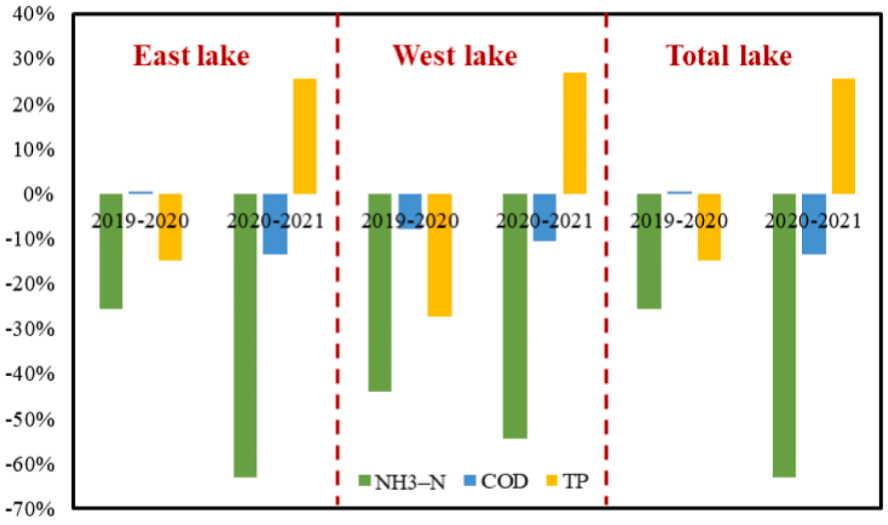

Fig.16. Year-over-year variance rate of NH3–N, COD and TP.

5. Conclusions

HABs outbreaks have been a global issue and pose a critical challenge to ecosystems and humans. This paper conducts a systematic spatio-temporal analysis framework of HABs variations based on a traditional algae-prone inland lake, Chaohu Lake. A total of 7926 MODIS remote sensing images were utilized to identify the distributions and trends of HABs from 2000 to 2021. Our results show that there had been an increasing general regime in HABs area and severity during the past two decades, and the duration within a year was generally increasing. Spatial analysis shows that the northern lake had severer HABs than the southern lake, especially the northwestern area, with consistently higher frequency and severity. Driving force analysis indicated that precipitation and temperature are two main dominant meteorological factors that positively correlated to HABs, and the fast-growing population and GDP of Hefei city are highly correlated to HABs increase since 2008. Water environment policies since 2020 significantly decreased water nutrients and HABs.

Furthermore, this study proved that high-frequency remote sensing observations, even with non-neglectable missing data caused by cloud cover, can still produce good performance in describing HABs dynamics. Although missing values may inevitably break the integrity of observation of a single image, they are still helpful in tracing the highly dynamic HABs trends because "imperfect data is better than no data". The current study may provide a potential reference for increasing remote sensing data utilizing efficiency in tracking highly dynamic objects.

Funding

This work was supported by the Natural Science Fund of China (Grant number U2243228); Natural Science Fund of Anhui Province (grant number 2008085ME158); Anhui Province Key Laboratory of Industrial Wastewater and Environmental Treatment (grant number ECEC-DHSZ202202).

CRediT authorship contribution statement

Ting Zhou: Conceptualization, Writing – original draft. **Yan Li:** Data curation, Investigation. **Bo Jiang:** Conceptualization, Methodology. **Juha M. Alatalo:** Writing – review & editing. **Chen Li:** Data curation, Investigation. **Cheng Ni:** Software.

Declaration of Competing Interest

The authors declare that they have no known competing financial interests or personal relationships that could have appeared to influence the work reported in this paper.

Data availability

Data will be made available on request.

Acknowledgments

This work is supported by National Natural Science Foundation of China (Grant number U2243228); Natural Science Fund of Anhui Province (Grant number 2008085ME158); Anhui Province Key Laboratory of Industrial Wastewater and Environmental Treatment (Grant number ECEC-DHSZ202202).

Appendix A. Supplementary data

Supplementary data to this article can be found online at https://doi.org/10.1016/j.ecolind.2022.109842.

References

Abbas, M.A., Iqbal, M., Tauqeer, H.M., Turan, V., Farhad, M., 2022. Chapter 16 - Microcontaminants in wastewater, in: Hashmi, M.Z., Wang, S., Ahmed, Z. (Eds.), Environmental Micropollutants, Advances in Pollution Research. Elsevier, pp. 315–329. https://doi.org/10.1016/B978-0-323-90555-8.00018-0.

Alikas, K., Kangro, K., Reinart, A., 2010. Detecting cyanobacterial blooms in large North European lakes using the Maximum Chlorophyll Index. oceanologia 52, 237–257. https://doi.org/10.5697/oc.52-2.237.

Bosse, K.R., Sayers, M.J., Shuchman, R.A., Fahnenstiel, G.L., Ruberg, S.A., Fanslow, D.L., Stuart, D.G., Johengen, T.H., Burtner, A.M., 2019. Spatial-temporal variability of in situ cyanobacteria vertical structure in Western Lake Erie: implications for remote sensing observations. J. Great Lakes Res. 45, 480–489. https://doi.org/10.1016/j.jglr.2019.02.003.

Box, W., Järvelä, J., Västilä, K., 2021. Flow resistance of floodplain vegetation mixtures for modelling river flows. J. Hydrol. 601, 126593 https://doi.org/10.1016/j.jhydrol.2021.126593.

Busico, G., Kazakis, N., Cuoco, E., Colombani, N., Tedesco, D., Voudouris, K., Mastrocicco, M., 2020. A novel hybrid method of specific vulnerability to anthropogenic pollution using multivariate statistical and regression analyses. Water Res. 171, 115386 https://doi.org/10.1016/j.watres.201 9.115386.

Cao, H.Y., Han, L., 2021. Hourly remote sensing monitoring of harmful algal blooms (HABs) in Taihu Lake based on GOCI images. Environ. Sci. Pollut. Res. Int. 28, 35958–35970. https://doi.org/10.1007/s11356-021-13318-6.

Cao, C.J., Zheng, B.H., Chen, Z.L., Huang, M.S., Zhang, J.L., 2011. Eutrophication and algal blooms in channel type reservoirs: a novel enclosure experiment by changing

light intensity. J. Environ. Sci. (China) 23, 1660–1670. https://doi.org/10.1016/s1001-0742 (10)60587-6.
Chen, C., Wang, Y., Chen, K., Shi, X., Yang, G., 2021. Using hydrogen peroxide to control cyanobacterial blooms: a mesocosm study focused on the effects of algal density in Lake Chaohu, China. Environ. Pollut. 272, 115923 https://doi.org/10.1016/j.envpol.2020.115923.
Cho, S., Lim, B., Jung, J., Kim, S., Chae, H., Park, J., Park, S., Park, J.K., 2014. Factors affecting algal blooms in a man-made lake and prediction using an artificial neural network. Measurement 53, 224–233. https://doi.org/10.1016/j.measurement.2014.03.044.
Coffer, M.M., Schaeffer, B.A., Salls, W.B., Urquhart, E., Loftin, K.A., Stumpf, R.P., Werdell, P.J., Darling, J.A., 2021. Satellite remote sensing to assess cyanobacterial bloom frequency across the United States at multiple spatial scales. Ecol. Indic. 128, 1–107822. https://doi.org/10.1016/j.ecoli nd.2021.107822.
Coffey, R., Paul, M., Stamp, J., Hamilton, A., Johnson, T., 2018. A review of water quality responses to air temperature and precipitation changes 2: nutrients, algal blooms, sediment, pathogens. J. Am. Water Resour. Assoc. 55, 844–868. https://doi.org/10.1111/1752-1688.12711.
Cong, D.U., Wang, S.X., Zhou, Y., Yan, F.L., 2009. Impact assessment of cyanobacteria bloom on water intakes in taihu lake using remote sensing data. China Environ. Sci. 29, 1041–1046. https://doi.org/10.3321/j.iss n:1000-6923.2009.10.007.
D'Silva, M.S., Anil, A.C., Naik, R.K., D'Costa, P.M., 2012. Algal blooms: a perspective from the coasts of India. Nat. Hazards 63, 1225–1253. https://doi.org/10.1007/s11069-012-0190-9.
DeVries, B., Huang, C., Armston, J., Huang, W., Jones, J.W., Lang, M.W., 2020. Rapid and robust monitoring of flood events using Sentinel-1 and Landsat data on the Google Earth Engine. Remote Sens. Environ. 240, 111664 https://doi.org/10.1016/j.rse.2020.111664.
Díaz, P.A., Peréz-Santos, I., Álvarez, G., Garreaud, R., Pinilla, E., Díaz, M., Sandoval, A., Araya, M., Álvarez, F., Rengel, J., Montero, P., Pizarro, G., López, L., Iriarte, L., Igor, G., Reguera, B., 2021. Multiscale physical background to an exceptional harmful algal bloom of Dinophysis acuta in a fjord system. Sci. Total Environ. 773, 145621 https://doi.org/10.1016/j.scitotenv.2021.145621.
Dong, Z., Xun, Y., Bao, S., Yu, D., Dong, L., Lin, H., Jin, Z., Yun, G., 2019. Using multi-source satellite imagery data to monitor cyanobacterial blooms of ChaohuLake. Infrared Laser Eng. 48, 726004. https://doi.org/10.3788/IRLA201948.0726004.
Duan, H.T., Loiselle, S.A., Zhu, L., Feng, L., Zhang, Y.C., Ma, R.H., 2015. Distribution and incidence of algal blooms in Lake Taihu. Aquat. Sci. 77, 9–16. https://doi.org/10.1007/s00027-014-0367-2.
Friedman, M.A., Levin, B.E., 2005. Neurobehavioral effects of harmful algal bloom (HAB) toxins: a critical review. J. Int. Neuropsychol. Soc. 11, 331–338. https://doi.org/10.1017/S13556177050503 81.
Gholizadeh, M.H., Melesse, A.M., Reddi, L., 2016. A comprehensive review on water quality parameters estimation using remote sensing techniques. Sensors (Basel) 16, E1298. https://doi.org/10.3390/s16081298.
Guo, H.L., Liu, H.Q., Lyu, H., Bian, Y.C., Zhong, S., Li, Y.Y., Song, M., Yang, Z.Q., Xu, J.F., Cao, J., Li, Y.M., 2022. Is there any difference on cyanobacterial blooms patterns between Lake Chaohu and Lake Taihu over the last 20 years? Environ. Sci. Pollut. Res. Int. 29, 40941–40953. https://doi.org/10.1007/s11356-021-18094-x.
Guo, X.N., Zhu, A.N., Chen, R.S., 2021. China's algal bloom suffocates marine life. Science 373, 751. https://doi.org/10.1126/science.abl5774.
He, S.Y., Ma, X.S., Wu, Y.L., 2018. Long Time Sequence Monitoring of Chaohu Algal Blooms Based on Multi-source Optical and Radar Remote Sensing, in: 2018 Fifth International Workshop on Earth Observation and Remote Sensing Applications (EORSA). In: Presented at the 2018 Fifth International Workshop on Earth Observation and Remote Sensing Applications (EORSA), pp. 1–5. https://doi.org/10.1109/EORSA.2018.8598609.
Hillman, C., Roundy, J., Kumar, S., Harris, T., Hosseini, A., 2021. Assimilation of Satellite Data for Predicting CyanoHABs in Kansas 2021, H35T-1274. https://ui.adsabs.harvard.edu/abs/2021 AGUFM.H35T1274H/abstract.
Hu, C.M., 2009. A novel ocean color index to detect floating algae in the global oceans. Remote Sens. Environ. 113, 2118–2129. https://doi.org/10.1016/j.rse.2009.05.012.
Hu, M.Q., Zhang, Y.C., Ma, R.H., Xue, K., Cao, Z.G., Chu, Q., Jing, Y.Y., 2021. Optimized remote sensing estimation of the lake algal biomass by considering the vertically heterogeneous chlorophyll distribution: Study case in Lake Chaohu of China. Sci. Total Environ. 771, 144811. https://doi.org/10.1016/j.scitotenv.2020.144811.
Huang, C.C., Li, Y.M., Yang, H., Sun, D.Y., Yu, Z.Y., Zhang, Z., Chen, X., Xu, L.J., 2014. Detection of algal bloom and factors influencing its formation in Taihu Lake from 2000 to 2011 by MODIS. Environ. Earth Sci. 71, 3705–3714. https://doi.org/10.1007/s12665-013-2764-6.
Hunter, P.D., Tyler, A.N., Gilvear, D.J., Willby, N.J., 2009. Using remote sensing to aid the assessment of human health risks from blooms of potentially toxic cyanobacteria. Environ. Sci. Technol. 43, 2627–2633. https://doi.org/10.1021/es802977u.
Jia, T.X., Zhang, X.Q., Dong, R.C., 2019. Long-term spatial and temporal monitoring of cyanobacteria blooms using MODIS on google earth engine: a case study in Taihu Lake. Remote Sens. 11, 2269. https://doi.org/10.3390/rs11192269.
Jing, Y.Y., Zhang, Y.C., Hu, M.Q., Chu, Q., Ma, R.H., 2019. MODIS-Satellite-based analysis of long-term temporal-spatial dynamics and drivers of algal blooms in a Plateau Lake Dianchi, China. Remote Sens. 11, 2582. https://doi.org/10.3390/rs11212582.
Johansen, K., Phinn, S., Taylor, M., 2015. Mapping woody vegetation clearing in Queensland, Australia from Landsat imagery using the Google Earth Engine. RSASE 1, 36–49. https://doi.org/1 0.1016/j.rsase.2015.06.002.
Khalil, M., Iqbal, M., Turan, V., Tauqeer, H.M., Farhad, M., Ahmed, A., Yasin, S., 2022. Chapter 11 - Household chemicals and their impact, in: Hashmi, M.Z., Wang, S., Ahmed, Z. (Eds.), Environmental Micropollutants, Advances in Pollution Research. Elsevier, pp. 201–232. https://doi.org/10.1016/B978-0-323-90555-8.00022-2.
Li, X.H., Jing, Y.H., Shen, H.F., Zhang, L.P., 2019. The recent developments in cloud removal approaches of MODIS snow cover product. Hydrol. Earth Syst. Sci. 23, 2401–2416. https://doi.org/10.5194/hess-23-2401-2019.
Li, H., Qin, C.X., He, W.Q., Sun, F., Du, P.F., 2021. Improved predictive performance of cyanobacterial blooms using a hybrid statistical and deep-learning method. Environ. Res. Lett. 16, 124045 https://doi.org/10.1088/1748-9326/ac302d.
Liu, E.F., Shen, J., Yang, X.D., Zhang, E.L., 2012. Spatial distribution and human contamination quantification of trace metals and phosphorus in the sediments of Chaohu Lake, a eutrophic shallow lake, China. Environ. Monit. Assess. 184, 2105–2118. https://doi.org/10.1007/s10661-011-2103-x.
Liu, H.T., Sun, K.X., Liu, X.Y., Yao, R., Cao, W.Z., Zhang, L., Wang, X.H., 2022. Spatial and temporal distributions of microplastics and their macroscopic relationship with algal blooms in Chaohu Lake, China. J. Contam. Hydrol. 248, 104028 https://doi.org/10.1016/j.jconhyd.2022.104028.
Liu, M.D., Wu, T., Zhao, X.Y., Zan, F.Y., Yang, G., Miao, Y.Q., 2021. Cyanobacteria blooms potentially enhance volatile organic compound (VOC) emissions from a eutrophic lake: field and experimental evidence. Environ. Res. 202, 111664 https://doi.org/10.1016/j.envres.2021.111664.
Lobo, F.de L., Nagel, G.W., Maciel, D.A., Carvalho, L.A.S.de, Martins, V.S., Barbosa, C.C.F., Novo, E.M.L. de M., 2021. AlgaeMAp: algae bloom monitoring application for inland waters in Latin America. Remote Sens. 13, 2874. https://doi.org/10.3390/rs13152874.
Ma, J.G., He, F., Qi, T.C., Sun, Z., Shen, M., Cao, Z.G., Meng, D., Duan, H.T., Luo, J.H., 2022. Thirty-four-year record (1987–2021) of the spatiotemporal dynamics of algal blooms in Lake Dianchi from multi-source remote sensing insights. Remote Sens. 14, 4000. https://doi.org/10.3390/rs14 164000.
Ma, J.Y., Jin, S.G., Li, J., He, Y., Shang, W., 2021. Spatio-temporal variations and driving forces of harmful algal blooms in Chaohu lake: a multi-source remote sensing approach. Remote Sens. 13, 427. https://doi.org/10.3390/rs13030427.
Marshall, M., Thenkabail, P., 2015. Advantage of hyperspectral EO-1 Hyperion over multispectral IKONOS, GeoEye-1, WorldView-2, Landsat ETM+, and MODIS vegetation indices in crop biomass estimation. ISPRS J. Photogramm. Remote Sens. 108, 205–218. https://doi.org/10.1016/j.isprsjprs.2015.08.001.
Mu, M., Wu, C.Q., Li, Y.M., Lyu, H., Fang, S.Z., Yan, X., Liu, G., Zheng, Z.B., Du, C.G., Bi, S., 2019. Long-term observation of cyanobacteria blooms using multi-source satellite images: a case study on a cloudy and rainy lake. Environ. Sci. Pollut. Res. Int. 26, 11012–11028. https://doi.org/10.1007/s11356-019-04522-6.
Naghdi, K., Moradi, M., Kabiri, K., Rahimzadegan, M., 2018. The effects of cyanobacterial blooms on MODIS-L2 data products in the southern Caspian Sea. Oceanologia 60, 367–377. https://doi.org/10.1016/j.oceano.2018.02.002.
Pan, M., K,Y., Zhao, X.D., Xu, Q.L., Peng, S.Y., L, H., 2012. Remote sensing recognition, concentration classification and dynamic analysis of cyanobacteria bloom in Dianchi Lake based on MODIS data, in: 2012 20th International Conference on Geoinformatics. Presented at the 2012 20th International Conference on Geoinformatics, IEEE, Hong Kong, China, pp. 1–5. https://doi.org/10.1109/Geoinformatics.2012.6270331.
Patil, J.S., Anil, A.C., 2008. Temporal variation of diatom benthic propagules in a monsoon-influenced tropical estuary. Cont. Shelf Res. 28, 2404–2416. https://doi.org/10.1016/j.csr. 2008. 06. 001.
Pyo, J., Cho, K.H., Kim, K., Baek, S.-S., Nam, G., Park, S., 2021. Cyanobacteria cell prediction using interpretable deep learning model with observed, numerical, and sensing data assemblage. Water Res. 203, 117483 https://doi.org/10.1016/j.watres.2021.117483.
Qin, X.M., Xia, W., Hu, X.X., Shao, Z., 2022. Dynamic variations of cyanobacterial blooms and their response to urban development and climate change in Lake Chaohu based on Landsat observations. Environ. Sci. Pollut. Res. Int. 29, 33152–33166. https://doi.org/10.1007/s11356-022-18616-1.
Shi, K., Zhang, Y.L., Qin, B.Q., Zhou, B.T., 2019. Remote sensing of cyanobacterial blooms in inland waters: present knowledge and future challenges. Sci. Bull. 64, 1540–1556. https://doi.org/10.1016/j.scib.2019.07.002.
Song, Z., Xu, W.X., Dong, H.L., Wang, X.W., Cao, Y.Q., Huang, P.J., Hou, D.B., Wu, Z.F., Wang, Z.Y., 2022. Research on cyanobacterial-bloom detection based on multispectral imaging and deep-learning method. Sensors 22, 4571. https://doi.org/10.3390/s22124571.
Stroming, S., Robertson, M., Mabee, B., Kuwayama, Y., Schaeffer, B., 2020. Quantifying the human health benefits of using satellite information to detect cyanobacterial harmful algal blooms and manage recreational advisories in U.S. Lakes. Geohealth 4. https://doi.org/10.1029/2020GH000254 e2020GH000254.
Sun, R.C., Yuan, H.L., Liu, X.L., Jiang, X.M., 2016. Evaluation of the latest satellite–gauge precipitation products and their hydrologic applications over the Huaihe River basin. J. Hydrol. 536, 302–319. https://doi.org/10.1016/j.jhydrol.2016.02.054.
Tamiminia, H., Salehi, B., Mahdianpari, M., Quackenbush, L., Adeli, S., Brisco, B., 2020. Google Earth Engine for geo-big data applications: a meta-analysis and systematic review. ISPRS J. Photogramm. Remote Sens. 164, 152–170. https://doi.org/10.1016/j.isprsjprs. 2020.04.001.
Teta, R., Sala, G.D., Esposito, G., Stornaiuolo, M., Scarpato, S., Casazza, M., Anastasio, A., Lega, M., Costantino, V., 2021. Monitoring cyanobacterial blooms during the COVID-19 pandemic in Campania, Italy: the case of Lake Avernus. Toxins 13, 471. https://doi.org/10.3390/toxins1307 0471.
Wang, S.L., Li, J.S., Zhang, B., Shen, Q., Zhang, F.F., Lu, Z.Y., 2016. A simple correction method for the MODIS surface reflectance product over typical inland waters in China. Int. J. Remote Sens. 37, 6076–6096. https://doi.org/10.1080/01431161.2016.1256508.

Wang, H.T., Wang, J.W., Liu, R.M., Yu, W.W., Shen, Z.Y., 2015. Spatial variation, environmental risk and biological hazard assessment of heavy metals in surface sediments of the Yangtze River estuary. Mar. Pollut. Bull. 93, 250–258. https://doi.org/10.1016/j.marpolbul.2015.01.026.

Xia, R., Zhang, Y., Wang, G.S., Zhang, Y.Y., Dou, M., Hou, X.K., Qiao, Y.F., Wang, Q., Yang, Z.W., 2019. Multi-factor identification and modelling analyses for managing large river algal blooms. Environ. Pollut. 254, 113056 https://doi.org/10.1016/j.envpol.2019.113056.

Xiong, X.X., Barnes, W., 2006. An overview of MODIS radiometric calibration and characterization. Adv. Atmos. Sci. 23, 69–79. https://doi.org/10.1007/s00376-006-0008-3.

Xu, F.-L., Tao, S., Dawson, R.W., Xu, Z.R., 2003. The distributions and effects of nutrients in the sediments of a shallow eutrophic Chinese lake. Hydrobiologia 492, 85–93. https://doi.org/10.1023/A:1024861727693.

Xu, Y.N., Xu, T.B., 2022. An evolving marine environment and its driving forces of algal blooms in the Southern Yellow Sea of China. Mar. Environ. Res. 178, 105635 https://doi.org/10.1016/j.marenvr es. 2022.105635.

Xue, K., Ma, R.H., Cao, Z.G., Shen, M., Hu, M.Q., Xiong, J.F., 2022. Monitoring fractional floating algae cover over eutrophic lakes using multisensor satellite images: MODIS, VIIRS, GOCI, and OLCI. IEEE Trans. Geosci. Remote Sens. 60, 1–15. https://doi.org/10.1109/TGRS.2022.3224 221.

Yuan, X.H., Shi, J.F., Gu, L.C., 2021. A review of deep learning methods for semantic segmentation of remote sensing imagery. Expert Syst. Appl. 169, 114417 https://doi.org/10.1016/j.eswa.2020.11 4417.

Zhang, Y.C., Ma, R.H., Zhang, M., Duan, H.T., Loiselle, S., Xu, J.D., 2015. Fourteen-year record (2000–2013) of the spatial and temporal dynamics of floating algae blooms in lake Chaohu, observed from time series of MODIS Images. Remote Sens. 7, 10523–10542. https://doi.org/10.3390/rs70810523.

Zhang, Y.C., Loiselle, S., Shi, K., Han, T., Zhang, M., Hu, M.Q., Jing, Y.Y., Lai, L., Zhan, P. F., 2021. Wind effects for floating algae dynamics in Eutrophic Lakes. Remote Sens. 13, 800. https://doi.org/10.3390/rs13040800.

Zhang, T.T., Hu, H., Ma, X.S., Zhang, Y.B., 2020. Long-term spatiotemporal variation and environmental driving forces analyses of algal blooms in Taihu Lake based on multi-source satellite and land observations. Water 12, 1035. https://doi.org/10.3390/w12041035.

Zhao, W., Duan, S.-B., 2020. Reconstruction of daytime land surface temperatures under cloud-covered conditions using integrated MODIS/Terra land products and MSG geostationary satellite data. Remote Sens. Environ. 247, 111931 https://doi.org/10.1016/j.rse.2020.111931.

Zhao, C.S., Shao, N.F., Yang, S.T., Ren, H., Ge, Y.R., Zhang, Z.S., Feng, P., Liu, W.L., 2019. Quantitative assessment of the effects of human activities on phytoplankton communities in lakes and reservoirs. Sci. Total Environ. 665, 213–225. https://doi.org/10.1016/j.scitotenv.2019.02.117.

Zhou, T., Ni, C., Zhang, M., Xia, P., 2022a. Assessing spatial and temporal distribution of algal blooms using gini coefficient and lorenz asymmetry coefficient. Front. Environ. Sci. 10 (10), 810902. https://www.frontiersin.org/articles/10.3389/fenvs.2022.810902.

Zhou, Z.-X., Yu, R.-C., Zhou, M.-J., 2022b. Evolution of harmful algal blooms in the East China Sea under eutrophication and warming scenarios. Water Res. 221, 118807 https://doi.org/10.1016/j.watres. 2022.118807.